Proc. Natl. Acad. Sci. USA
Vol. 95, pp. 15096–15101, December 1998
Physiology

Termination of Ca^{2+} release by a local inactivation of ryanodine receptors in cardiac myocytes

JAMES S. K. SHAM*†, LONG-SHENG SONG‡, YE CHEN‡, LI-HUA DENG*, MICHAEL D. STERN‡, EDWARD G. LAKATTA‡, AND HEPING CHENG†‡

*Division of Pulmonary and Critical Care Medicine, The Johns Hopkins Medical Institutions, Baltimore, MD 21224; and ‡Laboratory of Cardiovascular Science, Gerontology Research Center, National Institute on Aging, National Institutes of Health, Baltimore, MD 21224

Edited by Roger Y. Tsien, University of California, San Diego, CA, and approved October 10, 1998 (received for review July 14, 1998)

ABSTRACT **In heart, a robust regulatory mechanism is required to counteract the regenerative Ca^{2+}-induced Ca^{2+} release from the sarcoplasmic reticulum. Several mechanisms, including inactivation, adaptation, and stochastic closing of ryanodine receptors (RyRs) have been proposed, but no conclusive evidence has yet been provided. We probed the termination process of Ca^{2+} release by using a technique of imaging local Ca^{2+} release, or "Ca^{2+} spikes", at subcellular sites; and we tracked the kinetics of Ca^{2+} release triggered by L-type Ca^{2+} channels. At 0 mV, Ca^{2+} release occurred and terminated within 40 ms after the onset of clamp pulses (0 mV). Increasing the open-duration and promoting the reopenings of Ca^{2+} channels with the Ca^{2+} channel agonist, FPL64176, did not prolong or trigger secondary Ca^{2+} spikes, even though two-thirds of the sarcoplasmic reticulum Ca^{2+} remained available for release. Latency of Ca^{2+} spikes coincided with the first openings but not with the reopenings of L-type Ca^{2+} channels. After an initial maximal release, even a multi-fold increase in unitary Ca^{2+} current induced by a hyperpolarization to −120 mV failed to trigger additional release, indicating absolute refractoriness of RyRs. When the release was submaximal (e.g., at +30 mV), tail currents did activate additional Ca^{2+} spikes; confocal images revealed that they originated from RyRs unfired during depolarization. These results indicate that Ca^{2+} release is terminated primarily by a highly localized, use-dependent inactivation of RyRs but not by the stochastic closing or adaptation of RyRs in intact ventricular myocytes.**

In cardiac myocytes, Ca^{2+} release from sarcoplasmic reticulum (SR) is activated by the Ca^{2+}-induced Ca^{2+} release (CICR) mechanism (1–3). Recent evidence suggests that sarcolemmal L-type Ca^{2+} channels are closely associated with a cluster of sarcoplasmic Ca^{2+} release channels, called ryanodine receptors (RyRs), in the diadic junctions forming discrete release units (4–10). According to the "cluster bomb" model (11), Ca^{2+} influx via Ca^{2+} channels serves as the local Ca^{2+} signal to activate the coupled RyR(s), causing further increase in local [Ca^{2+}] and cross-activation of other RyRs within the release unit. These local release events have been visualized directly as "Ca^{2+} sparks" (12), and the recruitment of these events, as a function of Ca^{2+} channel activation and amplitude of unitary Ca^{2+} current (i_{Ca}), underlies the whole-cell Ca^{2+} transient induced by Ca^{2+} current (I_{Ca}) (13–15).

Despite improved understanding of the activation process, how Ca^{2+} release is terminated remains unclear. CICR, with its inherent positive feedback, is expected to operate in an "all-or-none" fashion. Regenerative activation of multiple RyRs within the release units should result in long-lasting Ca^{2+} sparks and unstable global Ca^{2+} oscillations. However, Ca^{2+} sparks of usually short duration (half-time of decay ≈22 ms) (12–14), and Ca^{2+} transients of graded amplitude and robust global stability occur in intact myocytes (16, 17), indicate that a regulatory mechanism(s) must exist to interrupt regenerative Ca^{2+} release. Several mechanisms have been proposed for the termination of Ca^{2+} release. (*i*) Ca^{2+}-induced inactivation of Ca^{2+} release (2, 18): Binding of released Ca^{2+} to an inactivation site of RyRs shifts the channels to an inactivated state and shuts off Ca^{2+} release. This was originally put forward by Fabiato (2), based on studies in skinned myocytes, as the mechanism to counteract CICR. However, this process has not been demonstrated in intact myocytes (19). (*ii*) Adaptation of RyRs (20–22): Spontaneous decline in open probability of RyR channels in lipid bilayers after activation by a step increase in [Ca^{2+}]; contrary to inactivation, the adapted channels can be reactivated by subsequent steps to higher [Ca^{2+}]. (*iii*) Stochastic attrition (11): Simultaneous stochastic closing of RyRs in an active release unit of a few RyRs, reducing local [Ca^{2+}] to a sub-threshold level and thereby extinguishing Ca^{2+} release. In addition, depletion or reduction of SR Ca^{2+} also may terminate Ca^{2+} release due to the lack of releasable Ca^{2+} or reduction in the gain of CICR (23, 24). To date, no conclusive supporting evidence has been provided for these putative mechanisms.

To elucidate the mechanistic nature of Ca^{2+} release termination, we applied a confocal-imaging technique (25), which enables both spatial and temporal resolution of local SR Ca^{2+} release fluxes, or "Ca^{2+} spikes", at the t-tubular-SR junctional regions during strong depolarizations, to track the kinetics of local Ca^{2+} release; and we made use of the Ca^{2+} channel agonist FPL64176 (FPL) and specific voltage-clamp protocols to manipulate the properties of single Ca^{2+} channel currents for triggering Ca^{2+} release. We tested specifically (*i*) whether increasing open-duration and enhancing reopenings of Ca^{2+} channels prolongs Ca^{2+} release and triggers secondary Ca^{2+} release, respectively, (*ii*) whether the SR Ca^{2+} is depleted after a maximal Ca^{2+} release induced by I_{Ca}, and (*iii*) whether RyRs can be reactivated by a stronger Ca^{2+} stimulus immediately subsequent to a prior activation. Our results provide direct evidence indicating that Ca^{2+} release is terminated mainly by a use-dependent inactivation of RyRs, whereas stochastic closing or adaptation of RyRs, or depletion of SR Ca^{2+} is not the primary cause of release termination in intact ventricular myocytes.

MATERIALS AND METHODS

Single Channel Recordings. Ventricular myocytes were enzymatically isolated from adult male Wistar rats (200–250

The publication costs of this article were defrayed in part by page charge payment. This article must therefore be hereby marked "*advertisement*" in accordance with 18 U.S.C. §1734 solely to indicate this fact.

This paper was submitted directly (Track II) to the *Proceedings* office.
Abbreviations: RyRs, ryanodine receptors; SR, sarcoplasmic reticulum; CICR, Ca^{2+}-induced Ca^{2+} release; FPL, Ca^{2+} channel agonist, FPL64176; OG-5N, Oregon Green 488 BAPTA-5N; i_{Ca}, unitary Ca^{2+} current; I_{Ca}, whole-cell Ca^{2+} current.
†To whom reprint requests should be addressed. e-mail: jsks@welchlink.welch.jhu.edu or chengp@grc.nia.nih.gov.

g). Cell-attached, patch-clamp recordings of L-type Ca^{2+} channels were obtained by using Sylgard (Dow Corning Midland, MI)-coated, thick-walled borosilicate glass pipettes (5–7 MΩ). Pipettes were filled with solution contained (in mM): 0.01 FPL, 10 $CaCl_2$, 130 tetraethylammonium chloride (TEA-Cl), and 10 Hepes (pH 7.4). Cells were bathed in high [K] solution, contained (in mM): 110 potassium aspartate, 30 KCl, 1 $MgCl_2$, 5 Hepes, 5 EGTA, and 3 Na_2ATP, pH 7.4, (free $[Ca^{2+}]$ = 100 nM) to approximately zero the membrane potential and enabled estimation of transpatch potentials. Unitary currents were recorded by using a cooled capacitor-feedback headstage (CV203B) and Axopatch 200B amplifier (Axon Instruments, Foster City, CA), low pass-filtered at 1 kHz, and digitized at 10 kHz. Data were collected and analyzed by using the pCLAMP software (Axon Instruments).

Simultaneous Measurement of I_{Ca} and SR Ca^{2+} Release Fluxes. Myocytes were whole-cell voltage clamped with patch pipettes with tip resistance of 1.5–2.5 MΩ, and superfused with Tyrode's solution containing (in mM): 137 NaCl, 2 $CaCl_2$, 5.4 KCl, 1 $MgCl_2$, 10 glucose, and 10 Hepes at pH 7.4, with 20 μM tetrodotoxin to block the sodium current. Membrane currents were measured with an Axopatch 200B patch-clamp amplifier. SR Ca^{2+} release fluxes were detected simultaneously with a novel laser confocal-imaging technique (25), by using the low affinity Ca^{2+} sensitive dye, Oregon Green 488 BAPTA-5N (OG-5N, Molecular Probes) in conjunction with high [EGTA], to minimize the resident time of free-released Ca^{2+} in the cytoplasm and to optimize the detection of localized high $[Ca^{2+}]$ in the release sites. The pipette solution contained (in mM): 105 CsCl, 10 NaCl, 5 MgATP, 10 Hepes, 20 TEA-Cl, 4 EGTA, 2 $CaCl_2$, and 1 OG-5N at pH 7.2, to eliminate K^+ currents and buffer-free $[Ca^{2+}]$ at 150 nM for adequate Ca^{2+} loading of SR. EGTA (4 mM) has no significant effect on the local Ca^{2+} signaling between L-type Ca^{2+} channels and RyRs (9). Confocal images were acquired by using a Zeiss LSM-410 inverted confocal microscope with a Zeiss Plan-Neofluor 40x oil immersion objective (NA = 1.3), and the confocal pinhole was set to render spatial resolutions of 0.4 μm in the *x–y* axis and 0.9 μm in the *z*-axis. OG-5N was excited by the 488 nm line of an argon laser, and fluorescence was measured at >515 nm. Images were taken in the line-scan mode, with 512 pixels/line (0.104 μm/pixel) scanned at 2.09 ms intervals, and processed by using IDL software (Research System, Boulder, CO). Conventional whole-cell Ca^{2+} transients were performed in some myocytes with methods described previously (9). All external solutions bathing the myocytes were exchanged rapidly (≈200 ms) with a concentration-clamp system to avoid changes in SR loading, and caffeine was rapidly applied by using a picospritzer. All experiments were performed at room temperature (20–22°C).

Data Analysis. Single Ca^{2+} channel records were leak and capacitive current eliminated by subtracting the original traces with blank sweeps. Open events were idealized by half-height criteria, and single channel patches were verified by the absence of stacked openings in entire data sets (>900 sweeps). Amplitudes of i_{Ca} were estimated from the Gaussian distributions of single channel currents, and open-time distribution was fitted with a bi-exponential probability distribution function. Latency distributions and averaged currents of the first openings and reopenings of Ca^{2+} channels were constructed from idealized events. Ca^{2+} release-induced inactivation of I_{Ca} was quantified as the fraction of peak I_{Ca} at 25 ms of clamp pulses ($I_{25\ ms}/I_{peak}$) and compared before and after complete depletion of SR Ca^{2+} with 10 mM caffeine. SR Ca^{2+} release fluxes were determined from line-scan confocal images as described by Song *et al.* (25). Briefly, spatially averaged OG-5N fluorescent signals from confocal images were normalized with basal fluorescence and expressed as F/F_0. The change in the OG-5N signal ($\Delta F/F_0$), in the presence of high EGTA concentration, is the sum of two components, a prominent spike component directly related to SR Ca^{2+} release fluxes (f_r), and a small pedestal component (f_s) representing the weighted

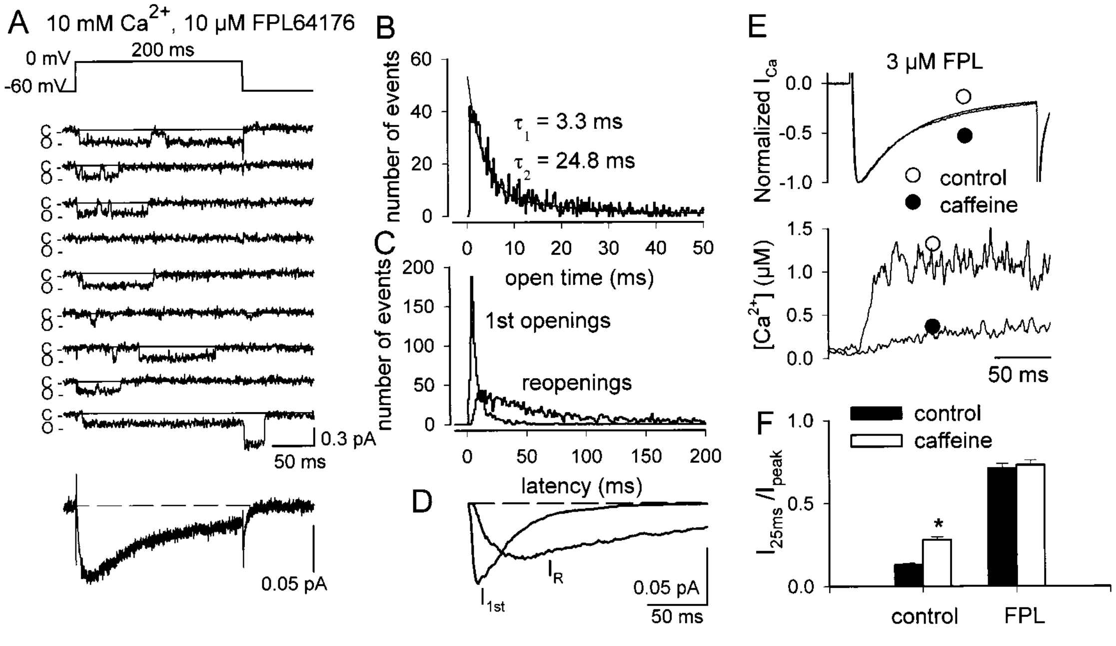

FIG. 1. FPL increases open probability, prolongs open duration, and prevents Ca^{2+} release-induced inactivation of Ca^{2+} channel. (*A*) Representative traces of unitary Ca^{2+} current recorded from a single channel patch at 0 mV, using 10 mM Ca^{2+} as the charge carrier in the presence of 10 μM FPL. (*A Bottom*) the ensemble averaged current of 925 sweeps. Notice the prolonged openings and reopenings during the pulse. (*B*) Open-time histogram of 1,907 opening events, bin width = 0.4 ms. The smooth line represents the best-fitted probability distribution function and τs denote the time constants. (*C*) Latency distribution of the first openings and reopenings of Ca^{2+} channel, bin width = 1 ms. Number of first openings is 637 and reopenings is 1,270. (*D*) Currents of the first opening (I_{1st}) and reopenings (I_R) of Ca^{2+} channels, reconstructed from idealized events. (*A* to *D*) Generated from the same patch. (*E*) Whole-cell I_{Ca} and Ca^{2+} transients in the presence of 3 μM FPL, before and during superfusion of 10 mM caffeine. (*F*) Inactivation of whole-cell I_{Ca}, quantified as $I_{25\ ms}/I_{peak}$, before and during superfusion of 10 mM caffeine, in control and FPL-treated (n = 13) myocytes. *, Significant difference from control ($P < 0.05$).

running integral of the release fluxes, thus $\Delta F/F_0 = f_r + f_s$, where $f_s = \alpha \int f_r dt$. f_s and α were determined experimentally by fitting f_s to the pedestal level of $\Delta F/F_0$ after repolarization, at which Ca^{2+} release was expected to be zero. f_r was then generated by subtracting f_s from the $\Delta F/F_0$ trace. Numerical simulation by using realistic buffer kinetics and concentrations showed that Ca^{2+} spikes reproduced well the waveform of Ca^{2+} fluxes, with an "on" and "off" response time of <1 ms, and the amplitude of the spike was linearly related to Ca^{2+} release flux over a wide range (25). All data were expressed as mean ± SEM and were compared by using paired *t* tests. *P* values <0.05 were considered statistically significant.

RESULTS AND DISCUSSIONS

Stochastic Closing of RyRs and Termination of SR Ca^{2+} Release. Previous numerical analysis of whole-cell Ca^{2+} transients (26, 27) and our recent direct measurement of SR Ca^{2+} release fluxes (25) revealed that Ca^{2+} release occurs and terminates shortly after the onset of a depolarizing pulses. Because L-type Ca^{2+} channel openings are brief (28–30), and reopenings of Ca^{2+} channels are inhibited to a large extent by the inactivation induced by Ca^{2+} release from SR (8–10) and Ca^{2+} influx via Ca^{2+} channels (29, 30), the transient nature of SR Ca^{2+} release may simply reflect the random stochastic closing of RyRs in the absence of a sustained trigger (11). In this scenario, an increase in the open duration of Ca^{2+} channels should provide a more prolonged stimulus to sustain the regenerative activation of RyRs; and reopenings of Ca^{2+} channels after release termination should provide new stimuli to reactivate the extinguished RyRs. To test this paradigm, the Ca^{2+} channel agonist FPL64176 (FPL) (31, 32) was used to prolong the open duration and enhance the reopenings of Ca^{2+} channels. Fig. 1 shows single Ca^{2+} channel currents recorded under cell-attached mode with Ca^{2+} (10 mM) as the charge carrier in the presence of FPL (10 μM). After depolarization to 0 mV, the probability of an active sweep was 0.60 ± 0.05, and open probability (P_o) of the active sweeps was 0.28 ± 0.04 (n = 3). The high P_o was mainly due to a prolonged open lifetime (mean open time = 15.9 ± 2.9 ms, n = 3 patches) (Fig. 1 *A* and *B*), which was ≈2 orders of magnitude longer than those recorded without FPL (mean open-time = 0.27 ms) (28). Latency distributions show that the first openings dominated the first 10 ms, and reopenings of Ca^{2+} channels constituted virtually all of the events after 30 ms of the clamp pulse, giving rise to the prominent maintained phase of I_{Ca} (Fig. 1 *C* and *D*). Additionally, FPL abolished the inactivation of Ca^{2+} channel

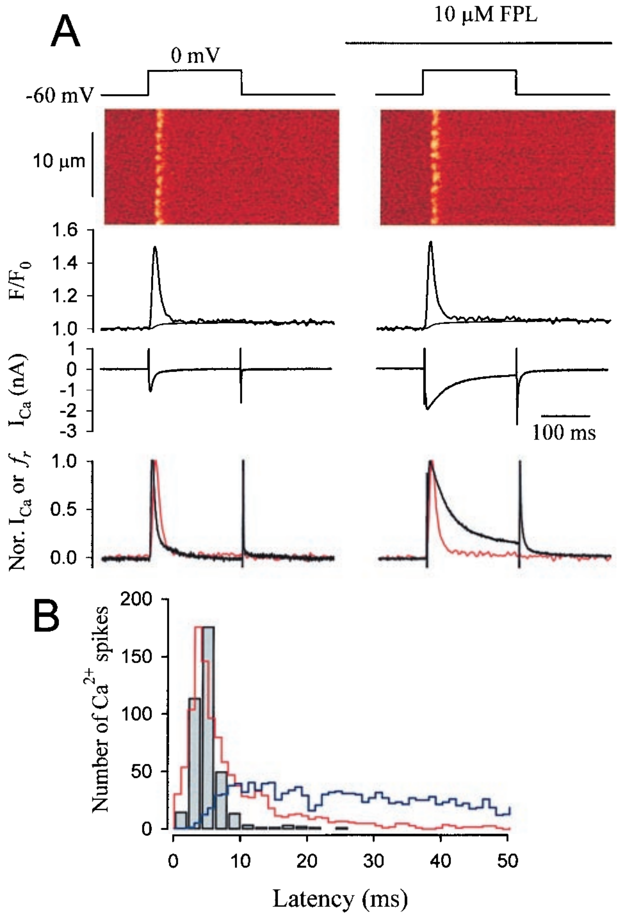

FIG. 2. Effect of FPL on SR Ca^{2+} release. (*A*) Ca^{2+} release immediately before (*Left* column) and during the first depolarizing pulse (*Right* column) after application of 10 μM FPL. From *Top* to *Bottom*: voltage protocols, confocal line-scan images, normalized spatially averaged OG-5N signals (F/F_0), I_{Ca}, and superimposed peak normalized I_{Ca} (black traces) and SR Ca^{2+} release function (f_r, red traces). Vertical and horizontal axes of line-scan images are axes of space and time, respectively. Smooth lines in the F/F_0 panels represent f_s and red lines in the *Bottom* panels represent f_r generated by subtracting f_s from the $\Delta F/F_0$ traces. (*B*) Latency distribution of Ca^{2+} spikes (n = 376) elicited in 10 myocytes during the first and second pulses after application of FPL (10 μM). The red and blue lines are the scaled latency distributions of the first openings and reopenings, respectively, of Ca^{2+} channel of Fig. 1*C*.

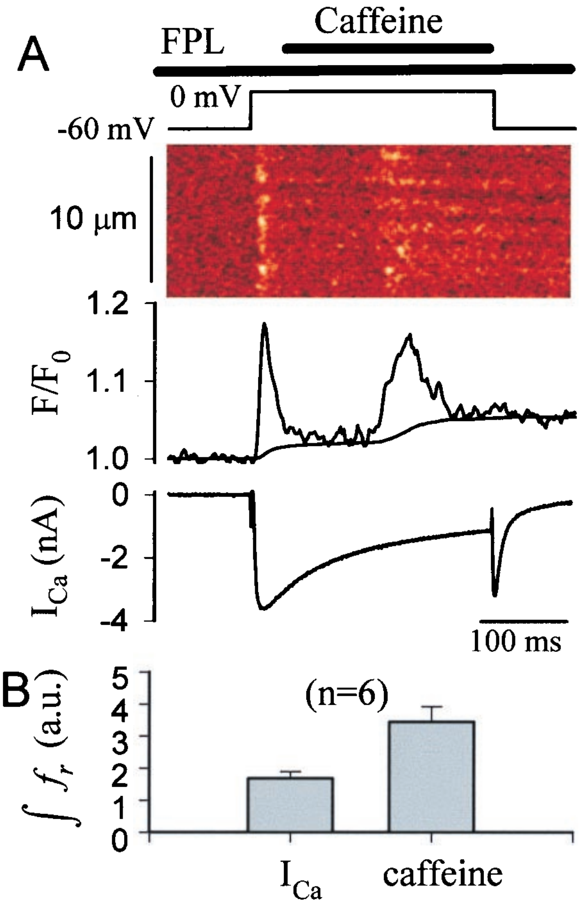

FIG. 3. Caffeine-induced Ca^{2+} release during the maintained phase of I_{Ca}. (*A Top* to *Bottom*) voltage protocol, confocal line-scan image, spatially averaged OG-5N fluorescence signal, and the simultaneously measured I_{Ca}. FPL (10 μM) was applied 10 s before depolarization, and caffeine was rapidly injected onto the cell 40 ms after the onset of depolarization. The smooth line in the *Middle* panel represents f_s. (*B*) Amount of SR Ca^{2+} released by I_{Ca} and caffeine quantified by integrating their respective release fluxes (f_r) transients (n = 6).

induced by Ca^{2+} release. Under control conditions, whole-cell I_{Ca} elicited at 0 mV inactivated rapidly ($I_{25\ ms}/I_{peak}$ = 0.13 ± 0.01, n = 13); the rate of inactivation was significantly reduced when SR Ca^{2+} release was abolished by 10 mM caffeine ($I_{25\ ms}/I_{peak}$ = 0.28 ± 0.02, $P < 0.05$). In the presence of FPL, inactivation of I_{Ca} was prolonged significantly ($I_{25\ ms}/I_{peak}$ = 0.71 ± 0.03, n = 13); inhibition of Ca^{2+} release with caffeine had minimal effect on the maintained phase and the rate of inactivation of I_{Ca} ($I_{25\ ms}/I_{peak}$ = 0.73 ± 0.03, n = 13) (Fig. 1 *E* and *F*). Reopenings of Ca^{2+} channels, thus, were not prevented by Ca^{2+} release triggered by their own first openings in the presence of FPL and provided multiple stimuli to the coupled RyRs during a depolarizing pulse.

Confocal images of SR Ca^{2+} release fluxes showed that depolarizations to 0 mV activated spatially discrete, localized Ca^{2+} spikes, which occurred and terminated within 40 ms after the onset of clamp pulse (Fig. 2*A*). They usually occurred only once at each release site (≈1.8 μm apart), without reactivation during the later part of depolarization. Estimations based on anatomical data (5, 33, 34) suggest that a resolvable volume (0.144 μm^3) of confocal images encompasses multiple diadic junctions; hence, a Ca^{2+} spikes represents the ensemble Ca^{2+} release fluxes originated from multiple release units within the same site. Rapid application of FPL (10 μM, 10 s before a clamp-pulse) caused an immediate enhancement of I_{Ca} (I_{peak} = 0.92 ± 0.11 nA in control and 3.64 ± 0.34 nA in FPL, n = 10, $P < 0.05$), a slowing of its inactivation, and an increase in the spatially averaged release transient ($\Delta F/F_0$ = 0.18 ± 0.02 in control, and 0.23 ± 0.02 in FPL, n = 10, $P < 0.05$). Surprisingly, the time course of Ca^{2+} release was unaltered (time to peak = 17.2 ± 1.2 ms in control and 15.2 ± 0.9 ms in FPL; time to 75% relaxation = 35.9 ± 2.1 ms in control and 34.2 ± 2.6 ms in FPL, n = 10); and no major secondary Ca^{2+} release was observed despite the presence of a prominent maintained I_{Ca}. The disparity between the kinetics of I_{Ca} and Ca^{2+} release is illustrated by superimposing the peak normalized I_{Ca} and spatially averaged Ca^{2+} release transients (Fig. 2*A Right Bottom*). These results were confirmed by using the first derivative of "conventional" Indo-1 Ca^{2+} transient (d[Ca^{2+}]/dt), as an empirical indicator of Ca^{2+} release (data not shown). Latency analysis shows that the occurrence of Ca^{2+} spikes, mostly within 2–10 ms of depolarization, coincided with the first latency of Ca^{2+} channels, but was completely dissociated from Ca^{2+} channel reopenings (Fig. 2*B*). These results argue against the stochastic attrition (11) as the primary mechanism for terminating Ca^{2+} release, because it predicts an increase in open duration of L-type Ca^{2+} channel would prolong Ca^{2+} release, and multiple Ca^{2+} channel reopenings would simply give rise to multiple release events. Moreover, the finding that Ca^{2+} release at 0 mV was activated exclusively by the first openings of Ca^{2+} channels (35) is consistent with the previous finding that Ca^{2+} release is gated by the initial phase of I_{Ca} (7, 14, 26, 27, 31, 36), but is in contrast to the observation that the latency distribution of Ca^{2+} sparks in the presence of Ca^{2+} channel blocker resembles the time course of I_{Ca} (13, 15). In the latter case, however, only a few Ca^{2+} release units were triggered at the onset, hence leaving plenty of unfired RyRs for activation in the later part of depolarizing pulses.

Recovery of Ca^{2+} release also was examined by applying a second depolarizing pulse at different intervals (50–1200 ms) after a maximal initial release at 0 mV. An apparent absolute refractory period of ≈150 ms was observed, followed by a second phase of recovery of Ca^{2+} release with a half-time of ≈500 ms (data not shown), similar to the previous observation on the interactions of evoked Ca^{2+} release with Ca^{2+} waves (38). The refractory period after a maximal Ca^{2+} release was, hence, significantly longer than that following a spontaneous spark (≈30 ms) (39) generated by only a single/few RyRs.

SR Ca^{2+} Depletion and Termination of Ca^{2+} Release. The refractoriness of SR after a maximal Ca^{2+} release could be due to global or local depletion of SR Ca^{2+}. To explore this possibility, high concentration of caffeine was applied to myocytes, which was exposed to FPL for 10 s, via a picospritzer at 40 ms after depolarization to cause complete release of Ca^{2+} from the SR. The rapid injection of caffeine caused a large release of Ca^{2+} during the otherwise silent later period of the clamp pulse (Fig. 3*A*), with Ca^{2+} spikes occurring at sites activated by I_{Ca} before the caffeine application. The amount of

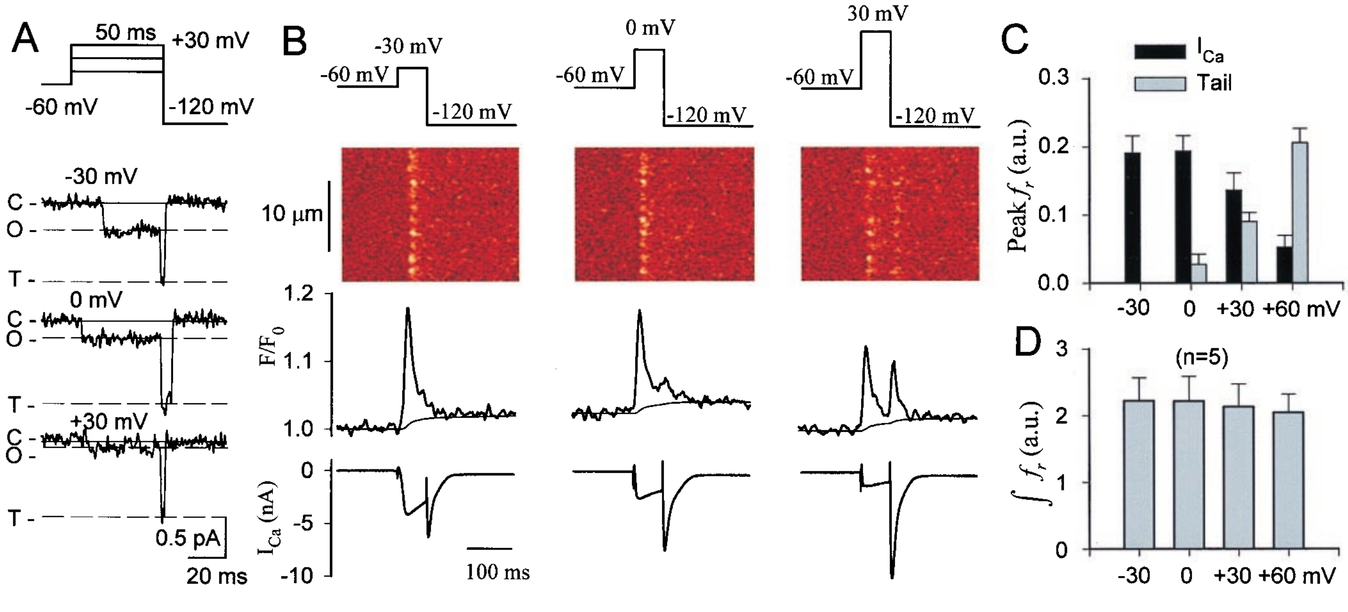

FIG. 4. Single channel current and SR Ca^{2+} release induced by depolarization and subsequent hyperpolarization. (*A*) Representative traces of single Ca^{2+} channel current recorded in the presence of 10 μM FPL, during depolarizing pulses (50 ms) to −30, 0, and +30 mV followed by hyperpolarizing steps to −120 mV. C, O, and T, mark the i_{Ca} when the channel was closed, open, and open during hyperpolarization (tail opening), respectively. Notice the multi-fold step increase in i_{Ca} upon hyperpolarization. (*B*) Representative line-scan images, spatially averaged OG-5N fluorescence signals and I_{Ca} simultaneously recorded in a myocyte. (*C*) Peak Ca^{2+} release fluxes elicited by a depolarizing pulse (to −30, 0, +30, or +60 mV, black bars) followed by a hyperpolarizing step (gray bars). (*D*) Cumulative Ca^{2+} release elicited by both depolarizing and hyperpolarizing pulses quantified by integrating f_r. Bar graphs *C* and *D* are the averaged data from five cells.

Ca^{2+} released by I_{Ca} compared with caffeine, quantified by integrating their respective release transients, had a ratio of 1:2.2 (Fig. 3*B*). Assuming the total releasable SR Ca^{2+} equals the sum of Ca^{2+} released by I_{Ca} and caffeine, the fractional release of Ca^{2+} induced by I_{Ca} was 33.1 ± 3.4% (n = 6), consistent with previous estimations (24, 40). This indicates that SR Ca^{2+} was not depleted after the initial release, and a substantial amount of Ca^{2+} was immediately available for release when RyRs were allowed to reopen. Moreover, the reduction of SR Ca^{2+} by one-third was unlikely the primary mechanism for the refractoriness of SR because I_{Ca} is able to trigger Ca^{2+} release after a similar reduction of Ca^{2+} loading (40), and Ca^{2+} release can be elicited within 2–3 depolarizing pulses immediately after complete depletion of SR by caffeine(9, 17, 40), suggesting that SR is capable of releasing Ca^{2+} with an even lower Ca^{2+} content (less than two-thirds of normal load). Moreover, spontaneous Ca^{2+} sparks were observed after 64% reduction in SR Ca^{2+} loading (41). However, the data do not exclude the possibility that the partial SR Ca^{2+} depletion may play a contributing role in terminating Ca^{2+} release by altering RyR activities (42, 43), and reducing the gain of CICR (24).

Inactivation vs. Adaptation of RyRs in Terminating SR Ca^{2+} Release. The refractoriness of SR to reopenings of L-type Ca^{2+} channels could be due to RyR adaptation or inactivation. To distinguish between these two possibilities, we devised a voltage-clamp protocol to test whether the once fired RyRs could be reactivated by a stronger Ca^{2+} stimulus, as would be predicted by the adaptation, but not by the inactivation hypothesis. Depolarizing pulses to either −30, 0, +30, or 60 mV were applied for 50 ms, followed by a hyperpolarization to −120 mV. Single channel recordings in the presence of FPL showed that i_{Ca} at −30, 0, and +30 mV were −0.42, −0.21, and −0.06 pA, respectively. Hyperpolarizing steps to −120 mV caused an instantaneous jump of i_{Ca} to −1.00 pA (Fig. 4*A*) due to an increase in the electrochemical gradient for Ca^{2+} influx. According to the adaptation hypothesis, the multi-fold increase in i_{Ca} during the hyperpolarizing steps should provide a local $[Ca^{2+}]$ sufficient to reactivate the adapted RyRs (20), even though these RyRs no longer respond to the smaller i_{Ca} of Ca^{2+} channel reopenings during depolarization. However, when this protocol was applied to intact myocytes, hyperpolarizing steps subsequent to the maximal Ca^{2+} releases elicited by depolarizations to −30 and 0 mV failed to trigger, or only activated a minimal Ca^{2+} release, despite the activation of a larger tail than initial I_{Ca} (Fig. 4 *B* and *C*). This result argues against the adaptation of RyRs but supports the hypothesis of strong inactivation of RyRs after their initial activation.

Yasui *et al.* (22) showed that depolarization to +30 mV, in the presence of FPL, elicits a transient Ca^{2+} release that terminates despite continued I_{Ca}, yet additional Ca^{2+} release is triggered by the tail current after repolarization; this has been interpreted as the evidence for adaptation of RyRs *in situ*. When our myocytes were first depolarized to +30 (or +60 mV) to activate a submaximal Ca^{2+} release, the subsequent hyperpolarizing step indeed triggered a "tail" release transient (Fig. 4*B Right*). However, the total amount of Ca^{2+} released by the depolarizing pulse and the subsequent hyperpolarizing step was similar to the maximal Ca^{2+} release at −30 or 0 mV (Fig. 4*D*), indicating that the large tail i_{Ca} did not trigger additional Ca^{2+} release from RyRs that fired during depolarization; rather, the tail transients likely represent the activation of release units that were not opened by the small i_{Ca} during the submaximal initial release. Because a Ca^{2+} spike is the ensemble release fluxes from multiple release units within a junctional site, in the latter case, the tail currents should elicit larger Ca^{2+} spikes in junctional sites where only a few release units were activated by the preceding depolarizing pulse, and trigger smaller Ca^{2+} release in sites where most of the release units were fired during the initial activation. Indeed, such a complementary release pattern was apparent at individual junctional sites: large initial Ca^{2+} spikes were often followed by either no or small tail releases at the same sites (Fig. 5*A*, sites 2, 4, and 6), whereas small or no initial releases were usually associated with larger tail Ca^{2+} spikes (Fig. 5*A*, sites 1, 3, and 5). Quantitatively, the amplitude of the initial Ca^{2+} spikes, elicited in 34 different release sites, correlated negatively ($r = -0.44$, $n = 170$, $P < 0.001$) with the tail Ca^{2+} spikes (Fig. 5*B*). These results clearly indicate that the large tail Ca^{2+} spikes were not generated by the reactivation of adapted RyRs because they were originated from sites where the initial activation of RyR was absence or minimal. The tail current failed to elicit secondary Ca^{2+} spikes from sites of large initial release further supports the inactivation of once activated RyRs at subcellular release sites.

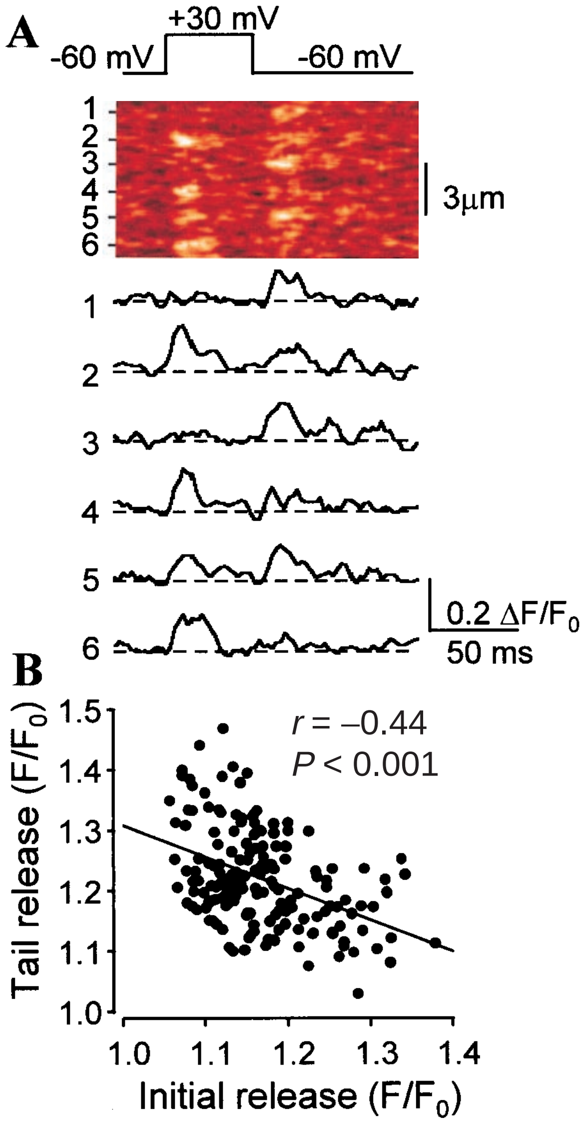

FIG. 5. Local Ca^{2+} release transients elicited at individual t-tubular-SR junctional sites in the presence of 10 μM FPL. (*A*) Confocal line-scan image (*Upper*) and Ca^{2+} spikes (*Lower*) elicited by a single depolarizing pulse to +30 mV for 50 ms, followed by repolarization to −60 mV. Numbers in the image indicate the spatial locations of the six individual release sites at which the Ca^{2+} spikes displayed in the *Lower* panel were recorded. (*B*) Scatter plot of amplitudes of depolarization-induced Ca^{2+} spikes vs. amplitudes of those triggered by the subsequent repolarization. The straight line is the least square linear regression of the data, r is the correlation coefficient, and n = 170.

Concluding Remarks. Using the imaging technique to directly measure SR Ca^{2+} release fluxes, in conjunction with the unique agonist, FPL64176, to manipulate the gating properties of L-type Ca^{2+} channels, we have provided compelling evidence that SR Ca^{2+} release during excitation–contraction coupling is terminated mainly by a local inactivation of RyRs in intact myocytes, whereas stochastic attrition, depletion of SR Ca^{2+}, and the adaptation of RyRs observed in lipid-layers (20, 21) do not participate or only play a contributing role in terminating Ca^{2+} release *in situ*. This inactivation of RyRs may depend on the high local $[Ca^{2+}]$consequential to their own Ca^{2+} release, as suggested previously in skinned fibers (2, 18), SR vesicles (44), and in single RyRs in lipid bilayers (45–47), as well as recently in intact myocytes (48), showing that the rate of Ca^{2+} spark termination is related to the magnitude of release flux. However, the possibility that the process is obligated to the activation of RyRs *per se* (49) cannot be excluded. Nevertheless, the inactivation process is highly localized, and use-dependent, and may be modulated, e.g., by cyclic adenosine monophosphate (21), Ca^{2+}/calmodulin-dependent protein kinases (50, 51), or FK506-binding protein (52–54). Because of this use-dependent inactivation, RyRs once activated are precluded from reactivation during a cardiac cycle; therefore, it interrupts the positive feedback of CICR, providing both global and micro-stability in cardiac myocytes. Since the mobilization of Ca^{2+} from intracellular stores through Ca^{2+} release channels is pivotal for signal transduction in many cell types, our findings as well as our experimental approaches may have important applications to studies of Ca^{2+} signaling in general.

We thank Dr. D. T. Yue for the valuable comments and Dr. H. Spurgeon and B. Ziman for the technical supports. This work was supported by the National Institutes of Health Intramural Research Programs (to H.C., M.D.S., and E.G.L.), extramural grant (HL-52652, to J.S.K.S.), and an American Heart Association Established Investigator award (to J.S.K.S.).

1. Fabiato, A. (1979) *Nature (London)* **281,** 146–148.
2. Fabiato, A. (1985) *J. Gen. Physiol.* **85,** 247–289.
3. Endo, M., Tanaka, M. & Ogawa, Y. (1970) *Nature (London)* **228,** 34–36.
4. Lewis-Carl, S., Felix, K., Caswell, A. H., Brandt, N. R., Ball, W. J., Jr., Vaghy, P. L., Meissner, G. & Ferguson, D. G. (1995) *J. Cell. Biol.* **129,** 673–682.
5. Sun, X.-H., Protasi, F., Takahashi, M., Takeshima, H., Ferguson, D. G. & Franzini-Armstrong, C. (1995) *J. Cell Biol.* **129,** 659–671.
6. Flucher, B. E. & Franzini-Armstrong, C. (1996) *Proc. Natl. Acad. Sci. USA* **93,** 8101–8106.
7. Wier, W. G., Egan, T. M., López-López, J. R. & Balke, C. W. (1994) *J. Physiol. (London)* **474,** 463–471.
8. Sham, J. S. K., Cleemann, L. & Morad, M. (1995) *Proc. Natl. Acad. Sci. USA* **92,** 121–125.
9. Sham, J. S. K. (1997) *J. Physiol.* **500,** 285–295.
10. Adachi-Akahane, S., Cleemann, L. & Morad, M. (1996) *J. Gen. Physiol.* **108,** 435–454.
11. Stern, M. D. (1992) *Biophys. J.* **63,** 497–517.
12. Cheng, H., Lederer, W. J. & Cannell, M. B. (1993) *Science* **262,** 740–744.
13. López-López, J. R., Shacklock, P. S., Balke, C. W. & Wier, W. G. (1995) *Science* **268,** 1042–1045.
14. Cannell, M. B., Cheng, H. & Lederer, W. J. (1995) *Science* **268,** 1045–1049.
15. Santana, L. F., Cheng, H., Gomez, A. M., Cannell, M. B. & Lederer, W. J. (1996) *Circ. Res.* **78,** 166–171.
16. Beuckelmann, D. J. & Wier, W. G. (1988) *J. Physiol.* **405,** 233–255.
17. Cleemann, L. & Morad, M. (1991) *J. Physiol.* **432,** 283–312.
18. Fabiato, A. (1992) *Adv. Exp. Med. Biol.* **311,** 245–262.
19. Näbauer, M. & Morad, M. (1990) *Am. J. Physiol.* **258,** C189–C193.
20. Györke, S. & Fill, M. (1993) *Science* **260,** 807–809.
21. Valdivia, H. H., Kaplan, J. H., Ellis-Davies, G. C. & Lederer, W. J. (1995) *Science* **267,** 1997–2000.
22. Yasui, K., Palade, P. & Györke, S. (1994) *Biophys. J.* **67,** 457–406.
23. Luo, C. H. & Rudy, R. (1994) *Circ. Res.* **74,** 1071–1113.
24. Bassani, J. W., Yuan, W. & Bers, D. M. (1995) *Am. J. Physiol.* **268,** C1313–C1329.
25. Song, L.-S., Sham, J. S. K., Lakatta, E. G., Stern, M. D. & Cheng, H. (1998) *J. Physiol.*, **51,** 677–691.
26. Sipido, K. R. & Wier, W. G. (1991) *J. Physiol.* **435,** 605–630.
27. Balke, C. W., Egan, T. M. & Wier, W. G. (1994) *J. Physiol. (London)* **474,** 447–462.
28. Rose, W. C., Balke, C. W. & Wier, W. G. (1992) *J. Physiol. (London)* **456,** 267–284.
29. Imredy, J. P. & Yue, D. T. (1994) *Neuron* **12,** 1301–1318.
30. Yue, D. T., Backx, P. H. & Imredy, J. P. (1990) *Science* **250,** 1735–1738.
31. Ramp, D. & Lacerda, A. E. (1991) *J. Pharmacol. Exp. Ther.* **259,** 982–987.
32. Kunze, D. L. & Rampe, D. (1992) *Mol. Pharmacol.* **42,** 666–670.
33. Forssmann, W. G. & Girardier, L. (1970) *J. Cell Biol.* **44,** 1–19.
34. Page, E. & Surdyk-Droske, M. (1979) *Circ. Res.* **45,** 260–267.
35. Isenberg, G. & Han, S. (1994) *J. Physiol.* **480,** 423–438.
36. Fabiato, A. (1985) *J. Gen. Physiol.* **85,** 291–320, 1985.
37. Cleemann, L., Wang, W. & Morad, M. (1998) *Proc. Natl. Acad. Sci. USA* **95,** 10984–10989.
38. Cheng, H., Lederer, M. R., Lederer, W. J. & Cannell, M. B. (1996) *Am. J. Physiol.* **270,** C148–C159.
39. Tanaka, H., Sekine, T., Kawanishi, T., Nakamura, R. & Shigenobu, K. (1998) *J. Physiol.* **508,** 145–152.
40. Trafford, A. W., Diaz, M. E., Negretti, N. & Eisner, D. A. (1997) *Circ. Res.* **81,** 477–484.
41. Song, L. S., Stern, M. D., Lakatta, E. G. & Cheng, H. (1997) *J. Physiol. (London)* **505,** 665–675.
42. Sitsapesan, R. & Williams, A. J. (1994) *J. Membr. Biol.* **137,** 215–226.
43. Lukyanenko, V., Gyorke, I. & Gyorke, S. (1996) *Pflügers Arch.* **432,** 1047–1054.
44. Meissner, G. & Henderson, J. S. (1987) *J. Biol. Chem.* **262,** 3065–3073.
45. Schiefer, A., Meissner, G. & Isenberg, G. (1995) *J. Physiol. (London)* **489,** 337–348.
46. Laver, D. R., Roden, L. D., Ahern, G. P., Eager, K. R., Junankar, P. R. & Dulhunty, A. F. (1995) *J. Membr. Biol.* **147,** 7–22.
47. Sitsapesan, R., Montgomery, R. A. & Williams, A. J. (1995) *Circ. Res.* **77,** 765–772.
48. Lukyanenko, V., Wiesner, T. F. & Gyorke, S. (1998) *J. Physiol. (London)* **507,** 667–677.
49. Laver, D. R. & Lamb, G. D. (1998) *Biophys. J.* **74,** 2352–2364.
50. Lokuta, A. J., Rogers, T. B., Lederer, W. J. & Valdivia, H. H. (1995) *J. Physiol.* **487,** 609–622.
51. Wang, J. & Best, P. M. (1992) *Nature (London)* **359,** 739–741.
52. Xiao, R. P., Valdivia, H. H., Bogdanov, K., Valdivia, C., Lakatta, E. G. & Cheng, H. (1997) *J. Physiol. (London)* **500,** 343–354.
53. McCall, E., Li, L., Satoh, H., Shannon, T. R., Blatter, L. A. & Bers, D. M. (1996) *Circ. Res.* **79,** 1110–1121.
54. Shou, W., Aghdasi, B., Armstrong, D. L., Guo, Q., Bao, S., Charng, M. J., Mathews, L. M., Schneider, M. D., Hamilton, S. L. & Matzuk, M. M. (1998) *Nature (London)* **391,** 489–492.